Available online at www.sciencedirect.com

SciVerse ScienceDirect

Ceramics International 38 (2012) 4601–4606

CERAMICS INTERNATIONAL

www.elsevier.com/locate/ceramint

Photoluminescence and LED application of β-SiAlON:Eu^{2+} green phosphor

Jun Ho Chung [a], Jeong Ho Ryu [b,*]

[a] Department of Materials Science and Engineering, Hanyang University, 17 Haengdang-dong, Seongdong-gu, Seoul 133-791, South Korea

[b] Department of Materials Science and Engineering, Korea National University of Transportation, 50 Daehak-ro, Chungju-si, Chungbuk 380-702, South Korea

Received 6 February 2012; accepted 15 February 2012

Available online 22 February 2012

Abstract

We successfully prepared β-SiAlON:Eu^{2+} phosphors with composition of $Eu_xSi_{6-z}Al_zO_yN_{8-y}$ ($y = z - 2x$, $x = 0.018$, $z = 0.23$) by gas-pressured synthesis for application to LED. The crystal phase, microstructure, PL emission and thermal quenching properties were investigated in detail. The β-SiAlON:Eu^{2+} phosphors absorbed broad UV–vis spectral region, and showed a single intense broadband emission near 538 nm. The Stokes shift and zero-phonon line were calculated mathematically, and also estimated from the spectral data. The β-SiAlON:Eu^{2+} green phosphor showed superior thermal quenching properties compared to commercial silicate ($SrBaSiO_4$:Eu^{2+}) green phosphor. The white light-emitting diode (LED) using the prepared β-SiAlON:Eu^{2+} green phosphor exhibited high color gamut, and good optical stability in high working temperature.

Keywords: A. Powders: solid state reaction; Photoluminescence; β-SiAlON:Eu^{2+}; Light-emitting diode

1. Introduction

Recently, rare-earth-doped oxynitride or nitride compounds have been reported to show photoluminescence properties and may then serve as new phosphors because of their good thermal and chemical stabilities [1–3]. Their luminescence properties are attributed to the strong nephelauxetic effect and large crystal field splitting effect [4]. Hirosaki et al. have developed a yellow oxynitride phosphor based on Eu^{2+}-doped Ca-α-SiAlON, and reported white LED devices using the yellow phosphor with a blue LED chip [5]. However, the white LEDs using the yellow phosphor presented relatively low color-rendering properties due to lack of enough green and red colors. Moreover, to improve the color reproducibility of back-lighting units (BLUs), appropriate green and red phosphors should be incorporated simultaneously. Therefore, it is necessary to develop highly luminescent green/red nitride/oxynitride phosphors using a simple solid-state synthetic method.

β-SiAlON has a hexagonal crystal structure ($P6_3$ or $P6_3/m$ space group), which is derived from β-Si_3N_4 structure by equivalent substitution of Al–O for Si–N, and its chemical composition can be written as $Si_{6-z}Al_zO_zN_{8-z}$ (z represents the number of Al–O pairs substituting for Si–N pairs and $0 < z \leq 4.2$) [6]. In a viewpoint of application to LEDs, phosphor materials must exhibit high phase purity, uniform crystal size distribution, high optical efficiency, high color stability and low thermal quenching property. In this work, Eu^{2+}-activated β-SiAlON phosphor with composition of $Eu_xSi_{6-z}Al_zO_yN_{8-y}$ ($y = z - 2x$, $x = 0.018$, $z = 0.23$ [7]) were successfully prepared via a simple solid-state synthetic route and its optical characteristics were analyzed in detail. Moreover, using a prepared β-SiAlON:Eu^{2+} green phosphor and a commercial $CaAlSiN_3$:Eu^{2+} red phosphor, we fabricated white LEDs for back-lighting unit (BLU), and their emission spectra were analyzed with working temperatures.

2. Experimental procedures

The β-SiAlON:Eu^{2+} green phosphor with composition of $Eu_xSi_{6-z}Al_zO_yN_{8-y}$ ($y = z - 2x$, $x = 0.018$, $z = 0.23$) was synthesized from α-Si_3N_4 (Ube Industries, Japan), AlN (Tokuyama, Japan) and Eu_2O_3 (Shin-Etsu, Japan) powders [8]. The Eu^{2+} (x value) and Al^{3+} doping concentrations (z value) were fixed at 0.018 and 0.23, respectively. The raw powder mixtures were prepared using a Si_3N_4 ball milling in n-hexane. After drying in vacuum oven, the powder mixture was granulated using a test sieve, and then loaded into a BN

* Corresponding author. Tel.: +82 43 841 5384; fax: +82 43 841 5380.
E-mail address: jhryu@ut.ac.kr (J.H. Ryu).

0272-8842/$36.00
doi:10.1016/j.ceramint.2012.02.039

crucible. Calcination was carried out at 2000 °C for 5 h in 0.90 MPa of N_2 atmosphere using GPS (gas pressured sintering) furnace. After heating, the power was shut off and the samples were cooled down in the GPS furnace. The crystalline phase of the synthesized powders were identified by X-ray powder diffraction (XRD), operating at 40 kV using Cu Kα radiation (λ = 1.5406 Å). The data were collected in the continuous scan mode at the speed of 3° at 2θ/min with step size of 0.02° from 10° to 80°. The powder morphology and microstructure were investigated by scanning electron microscopy (SEM). The photoluminescence (PL) properties of the prepared phosphor samples were measured using a spectrofluorometer in a temperature range from 25 to 250 °C with a 450 W xenon lamp as an excitation source. The excitation wavelength used for measuring PL emission was 450 nm, and the excitation spectra were measured at emission maxima. To fabricate white LEDs, the prepared β-SiAlON:Eu^{2+} green phosphor and a commercial $CaAlSiN_3$:Eu^{2+} red phosphor were mixed and then the mixed powder was blended with epoxy in order to be pre-coated on the LED chip. The emission spectra of the white LEDs were measured by the spectral/goniometric analyzer in a working temperature range from 25 to 150 °C.

3. Results and discussion

3.1. Synthesis and optical properties

Fig. 1(a) shows XRD pattern of the synthesized Eu^{2+}-doped β-SiAlON green phosphor powder with the composition of $Eu_xSi_{6-z}Al_zO_yN_{8-y}$ ($y = z - 2x$, $x = 0.018$, $z = 0.23$). The synthesized phosphor sample consists of a single β-SiAlON crystalline phase (JSPDS card No. 48-1615) without secondary SiAlON polytypoid phases (27R, 21R or 12H). It is well known that β-SiAlON comprises a three-dimensional network structure [9] of corner sharing (Si, Al)(O, N)$_4$ tetrahedra with continuous channels along [0 0 1] direction as represented in inset of Fig. 1(a). Typical SEM images of the synthesized Eu^{2+}-doped β-SiAlON green phosphor powder are presented with magnifying power of 3000 in Fig. 1(b) and 1000 in inset of (b). As shown, the Eu^{2+}-doped β-SiAlON powder had an elongated rod-like shape with a uniform size of 20–50 μm in length and 3–5 μm in diameter. From a viewpoint of practical application to LEDs, the prepared Eu^{2+}-doped β-SiAlON phosphor powder is enough to be applicable, because it has high phase purity, fine particle size and high uniformity without any irregular agglomerates as confirmed in XRD and SEM data.

Fig. 2(a) represents the excitation and emission spectra of the synthesized Eu^{2+}-doped β-SiAlON green phosphor measured at room temperature. The excitation spectrum monitored at the peak of emission spectrum covers a broad range from 350 to 500 nm. Two peaks near 360 and 405 nm are observed, which are assigned to $4f^7 \rightarrow 4f^6 5d^1$ absorption of the Eu^{2+} cations. The emission spectrum of the prepared β-SiAlON:Eu^{2+} phosphor excited at 450 nm, exhibits single broad band at 538 nm. The broad band is due to the allowed $4f^6 5d^1 \rightarrow 4f^7$ transition of Eu^{2+} [10]. No special emission peaks of Eu^{3+} (sharp lines between 580 and 650 nm) were observed in

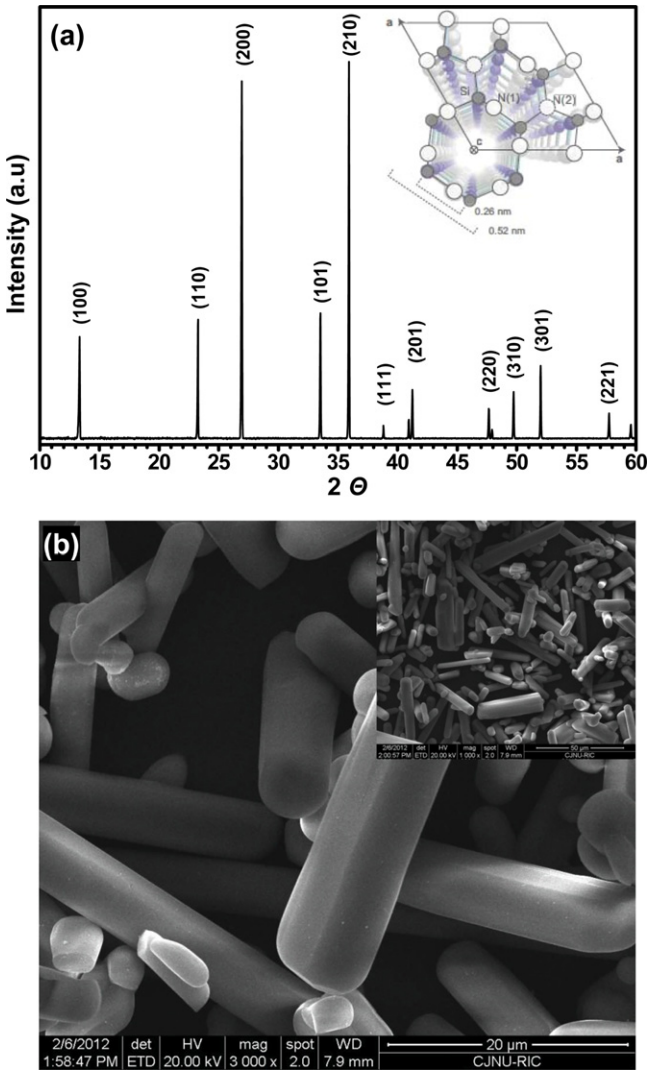

Fig. 1. (a) X-ray diffraction patterns of $Eu_xSi_{6-z}Al_zO_yN_{8-y}$ ($y = z - 2x$, $x = 0.018$, $z = 0.23$) prepared at 2000 °C for 5 h and schematic projection [9] of supercell in β-SiAlON structure onto the (0 0 1) plane. (b) Typical SEM figures for the Eu^{2+}-doped β-SiAlON green phosphor with magnifying power of 3000 and 1000 in inset of (b).

the spectrum, suggesting that Eu^{3+} was reduced to Eu^{2+} in the reducing nitrogen atmosphere [11]. The full width of half maximum (FWHM) value is about 50 nm, which is smaller than that of commercial green $SrBaSiO_4$:Eu^{2+} (∼65 nm) phosphor [12]. It is clearly confirmed that of Eu^{2+}-doped β-SiAlON phosphor can also be excited efficiently in a near-UV or blue-light region (350–460 nm). These results indicate that the prepared Eu^{2+}-doped β-SiAlON is promising down-conversion green phosphor material for solid-state lighting utilizing InGaN-based near-UV or blue chip LEDs.

The Stokes-shift of the prepared Eu^{2+}-doped β-SiAlON green phosphor with a composition of $Eu_xSi_{6-z}Al_zO_yN_{8-y}$ ($y = z - 2x$, $x = 0.018$, $z = 0.23$) was calculated mathematically and estimated from the PL spectral data. The classical description cannot satisfactorily explain emission spectral shapes and non-radiative transition probabilities. The single configuration coordinate model [13] based on quantum

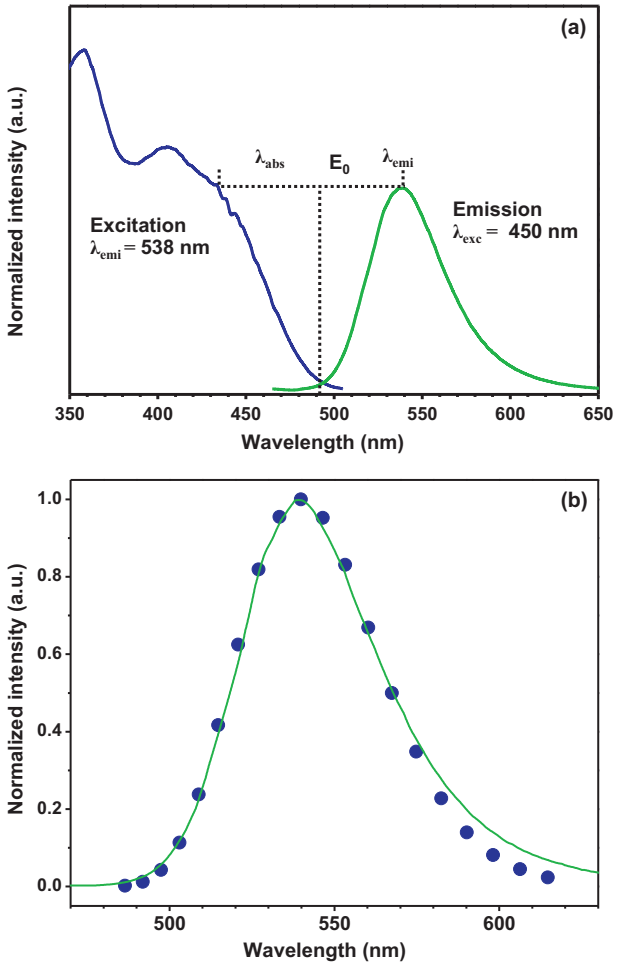

Fig. 2. (a) The room temperature excitation and emission spectra of the prepared Eu^{2+}-doped β-SiAlON green phosphor. (b) Experimental (solid line) and calculated (circles) emission spectrum at 25 °C under excitation at 450 nm.

mechanics was used to fit the emission band of considered phosphor. Because the 4f-shell is well shielded, the electron–vibrational interaction within this shell is negligible so that the intensities of the vibronic satellites corresponding to 4f–4f transitions are small. On the contrary, 4f–5d transitions give rise to the broad vibronic bands whose shape-function can be described by the normalized Pekarian type spectral distribution [14].

$$F(\Omega) = \exp\left[-\frac{a}{2}\coth\left(\frac{p\hbar\omega}{2kT}\right)\right]\sum_{-\infty}^{\infty}\exp\left(\frac{p\hbar\omega}{2kT}\right) I_p \cdot \left(\frac{a}{2\sinh(\hbar\omega/2kT)}\right)\delta(\Omega - \Omega_0 - p\omega) \quad (1)$$

In Eq. (1), $I_p(x)$ is the modified Bessel function that represents a series of the discrete lines, a is the so-called heat release parameter (shift of the dimensionless vibrational coordinate after photon absorption), $\delta(\Omega - \Omega_0 - p\omega)$ is the Dirac δ-function that describes an individual vibrational line of the dimensional frequency $p = (\Omega - \Omega_0)/\omega$, and Ω_0 is the frequency of the zero-phonon line, ω is the frequency of the active vibrational mode. If the dispersion zone of the lattice vibrations is taken into account, the shape function is smoothed that is achieved by replacing the δ-function by the Gaussian or Lorentzian bands. In the case of low temperature, Pekarian can be simplified. In this case, $\sinh(\hbar\omega/2kT) \approx (1/2)\exp(\hbar\omega/kT)$, $\exp(-a/2\coth\hbar\omega/2kT) \approx \exp(-a/2)$ and the modified Bessel function can be represented as a series in terms of the argument $a\,e^{-p\hbar\omega/2kT}$:

$$I_p(a\,e^{-(\hbar\omega/2kT)}) \approx \left[\left(\frac{a}{2}\right)^p\frac{1}{p!} + \left(\frac{a}{2}\right)^{p+2}\frac{1}{(p+1)!}e^{-(\hbar\omega/kT)}\right]e^{-(p\hbar\omega/2kT)} \quad (2)$$

In the decomposition (2) small terms $[a\,e^{-(\hbar\omega/2kT)}]^4$ (and high order terms) are neglected that is justified when the temperature is low enough ($kT \le \hbar\omega$) and the vibronic coupling is not too strong. Combining Eqs. (1) and (2) one can obtain the following low temperature approximation for the band profile of the vibronic band:

$$F(\Omega) = e^{-(a/2)}\left[\sum_{p=0}^{\infty}\left(\frac{a}{2}\right)^p\frac{1}{p!} + \sum_{p=-1}^{\infty}\left(\frac{a}{2}\right)^{p+2}\frac{1}{(p+1)!}e^{-(\hbar\omega/kT)}\right] \cdot \delta(\Omega - \Omega_0 - p\omega) \quad (3)$$

This expression describes a discrete set of the vibronic lines (each represented by a corresponding δ-function) and therefore reflects quantum properties of the vibrations. The dispersion of the vibrations smoothes the discrete structure and one can omit the δ-functions and the required summations. Therefore intensity of the band in Eq. (3) can be considered as a function of the continuous parameter p:

$$F(p) = e^{-(a/2)}\left[\left(\frac{a}{2}\right)^p\frac{1}{p!} + \left(\frac{a}{2}\right)^{p+2}\frac{1}{(p+1)!}e^{-(\hbar\omega/kT)}\right] \quad (4)$$

or we can rewrite (4) as follows:

$$F(n) = \frac{e^{-S}\cdot S^n}{n!}\left[1 + S^2\frac{1}{(n+1)}e^{-(\hbar\omega/kT)}\right] \quad (5)$$

where $S = a/2$ is the Huang–Rhys–Pekar factor – the number of emitted phonons accompanying the optical transition, n corresponds to one of the vibration level in the ground electronic state on which the vibronic transition is transferred from the fundamental vibrational level of the emitting electronic state ($n = 0$ is a zero-phonon line), ω is the frequency of the active vibrational mode, k the Boltzmann constant, and T is a given temperature. A plot of F against n gives an absorption spectrum consisting of many sharp lines. At temperature $T = 0$ K from this equation we obtain a well known transition probability given by a simple relation [13,14]:

$$F(n) = \frac{e^{-S}\cdot S^n}{n!} \quad (6)$$

Usually, only the first term in Eq. (1) that is the Poisson type distribution is taken into account in consideration of the band shapes at low temperatures. From the physical point of view, this means absorption (emission) originates from the fundamental vibronic level in the initial electron-vibrational state.

This approximation fails when the temperature is high enough, for example, room temperature, when the most PL measurements are carried out. Under this condition, the second term in Eq. (1) corresponding to the emission (absorption) from both ground and first excited levels is important and plays an important role. The application of Eq. (1) instead of Eq. (2) gives us more correct and more precise fitting of experimental results.

The temperature variation of the FWHM (full width of half maximum) can be described using the configuration coordinate model and the Boltzmann distribution according to the following equation:

$$\mathrm{FWHM}\,(T) = \sqrt{8 \cdot \ln 2} \cdot \hbar\omega \cdot \sqrt{S} \cdot \sqrt{\coth \frac{\hbar\omega}{2kT}} \tag{7}$$

where $\hbar\omega$ is the mean phonon energy, S the Huang–Rhys–Pekar parameter and k the Boltzmann constant. This equation can be used only when the parabolas of the ground state and the excited state have the same curvature. By combining Eq. (5) with (7) we obtained the best fits of the emission bands for the prepared $Eu_xSi_{6-z}Al_zO_yN_{8-y}$ ($y = z - 2x$, $x = 0.018$, $z = 0.23$) green phosphor powder with the Huang–Rhys–Pekar parameter $S = 10.15$ and phonon energy $\hbar\omega = 26.80$ meV, which are shown in Fig. 2(b).

In turn, the knowledge of Huang–Rhys–Pekar factor and phonon energy allows us to determine the Stokes shift. By supposing that the ground state parabola of the configuration coordinate model presents the same curvature as the excited state parabola, i.e. the phonon energy is the same for the $4f^7(^8S_{7/2})$ ground state as for the $4f^6(7F)5d$ excited state, we can determinate the Stokes shift (ΔS). ΔS is related to the offset of the parabolas in the configuration coordinate diagram and ΔS is equal to:

$$\Delta S = (2S - 1) \cdot \hbar\omega \tag{8}$$

We can apply this method to study synthesized Eu^{2+}-doped β-SiAlON green phosphor. For the synthesized green phosphor, the Stokes shift calculated from Eqs. (1), (3) and (4) is 4250 cm^{-1}. These data were compared with experimentally excitation and emission spectra. The main problem at room or higher temperatures is to determine correctly the λ_{abs}, because usually this wavelength is not resolved at room or higher temperatures. An almost mirror–image relationship seems to hold between the emission and the excitation spectra in the energy region between the two maxima, as shown in Fig. 2(a). This relation is characteristic of a phonon-broadened emission and confirms the hypothesis that the mean phonon energy $\hbar\omega$ is the same for the $4f^7(^8S_{7/2})$ ground state as for the $4f^6(^7F)5d$ excited state. We can determine the energy of the zero-phonon line E_0 at the intersection of the emission and excitation spectra. From Fig. 4(b), we found $E_0 = 492$ nm and Stokes shift $\Delta S = \lambda_{em} - \lambda_{abs} = 4310\ cm^{-1}$. As one can ascertain from this result, the mathematical calculation (4250 cm^{-1}) with consideration of the temperature dependence, is in good agreement with this experimental PL result.

3.2. Thermal quenching properties

The thermal quenching property is one of the most important parameters for applying phosphor to LEDs. For the application of white LEDs, phosphors with low thermal quenching have big advantage because most of the energy loss of LED is dissipated to heat, which induce the junction temperature of LED to increase up to 150 °C. Thus, small thermal quenching of phosphors is necessary for the stable optical properties and better lifetimes of LEDs [15]. The temperature-dependent PL properties of the prepared Eu^{2+}-doped β-SiAlON green phosphor was investigated in a temperature range from 25 to 250 °C, and the results are shown in Fig. 3(a). For comparing, commercial silicate green phosphor ($SrBaSiO_4:Eu^{2+}$) was measured in the same temperature region and the result is represented in inset of Fig. 3(a). Fig. 3(b) displays gradual changes of the normalized PL emission intensities for Eu^{2+}-doped β-SiAlON and silicate phosphor schematically. When the temperature was raised, the prepared Eu^{2+}-doped β-SiAlON

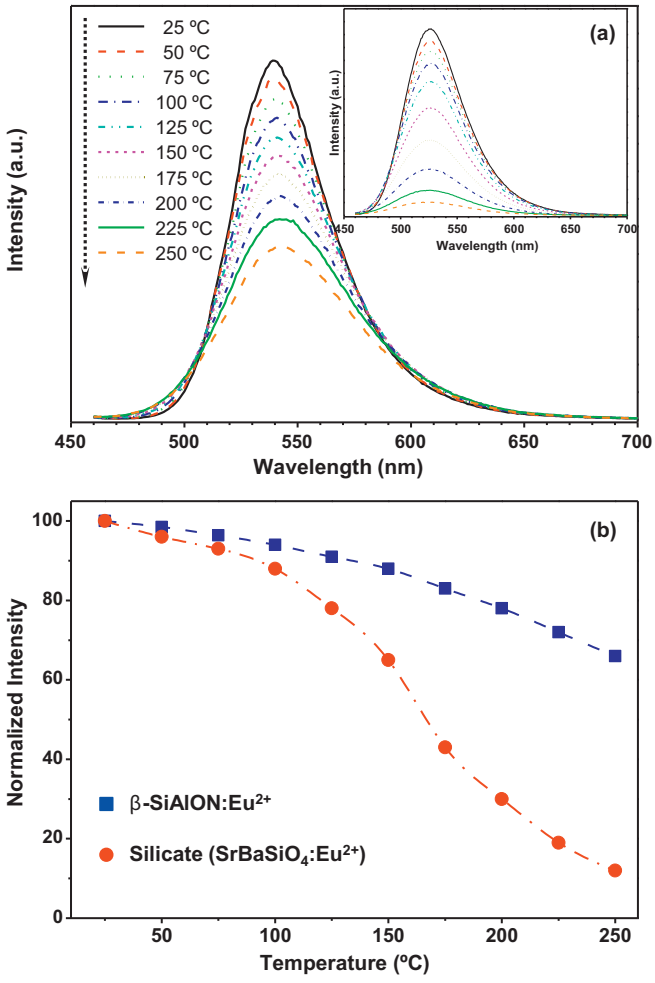

Fig. 3. (a) Temperature-dependent PL emission spectra of the prepared Eu^{2+}-doped β-SiAlON in a temperature range from 25 to 250 °C. For comparison, PL emission spectra of a commercial silicate green phosphor ($SrBaSiO_4:Eu^{2+}$) measured in the same temperature range were shown in inset. (b) The dependences of the PL intensity on the measuring temperatures are shown schematically.

green phosphor showed less decrease in emission intensity, which indicates a high thermal stability. This is a very important characteristic in white LEDs for achieving high optical stability at high temperatures. At 150 °C, the PL emission intensity of Eu^{2+}-doped β-SiAlON green phosphor was about 88% of room temperature, while the green $SrBaSiO_4:Eu^{2+}$ phosphor showed 65%. When the measured temperature is higher than 200 °C, the PL emission intensity of the silicate green phosphor ($SrBaSiO_4:Eu^{2+}$) was less than half of the Eu^{2+}-doped β-SiAlON green phosphor. Therefore, the thermal quenching results confirm that Eu^{2+}-doped β-SiAlON is promising green phosphor for LEDs in illumination, automobile and LCD TV applications.

3.3. LED application properties

Fig. 4 shows the emission spectra of white LEDs and the simulated spectra using LCD color filter for two types of the LED BLU with silicate ($SrBaSiO_4:Eu^{2+}$) (a) and β-SiAlON:Eu^{2+} (b) as a green phosphor, respectively. The $CaAlSiN_3:Eu^{2+}$ phosphor was used for a red phosphor in both cases. The RGB (red, green and blue) color coordinates (1976 CIE system) of the LED BLUs are shown for (c) commercial silicate and (d) β-SiAlON:Eu^{2+}, respectively. Obviously, the color purity of the green emission of LED BLU using β-SiAlON:Eu^{2+} is higher than that of LED BLU with green silicate phosphor. The color gamut of BLU using β-SiAlON:Eu^{2+} was 102% of NTSC, which is 6% higher than that of BLU using silicate phosphor. As shown in emission spectra of Fig. 4(a) and (b), the separation of blue and green spectrum is more clear in case of β-SiAlON:Eu^2 because it has narrower FWHM of emission spectrum (∼50 nm) than silicate green phosphor (∼64 nm). This accounts for the higher color gamut of the LED BLU using β-SiAlON:Eu^{2+} green phosphor.

The stabilities of optical power and chromaticity with working temperatures must be taken into account when BLU is designed for LCD monitors or TVs, because the thermal dissipation from active layer of LED chip under high current density can cause thermal quenching of phosphor, following by changes of optical power and chromaticity. Fig. 5 shows the variation of the normalized optical power of white LEDs using (a) silicate and (b) β-SiAlON:Eu^{2+} with respect to the working temperatures, respectively. In case of white LED with silicate green phosphor, considerable power-drops were measured from 75 °C, which gave rise to the gradual decrease in color indices as shown in Fig. 5(c). On the contrary, there was not a noticeable power-drop nor change of chromaticity in the case using β-SiAlON:Eu^{2+} green phosphor even at 150 °C. From these results, it can be expected that LED BLUs using β-SiAlON:Eu^{2+} as green phosphor could have much smaller drift of color coordinate

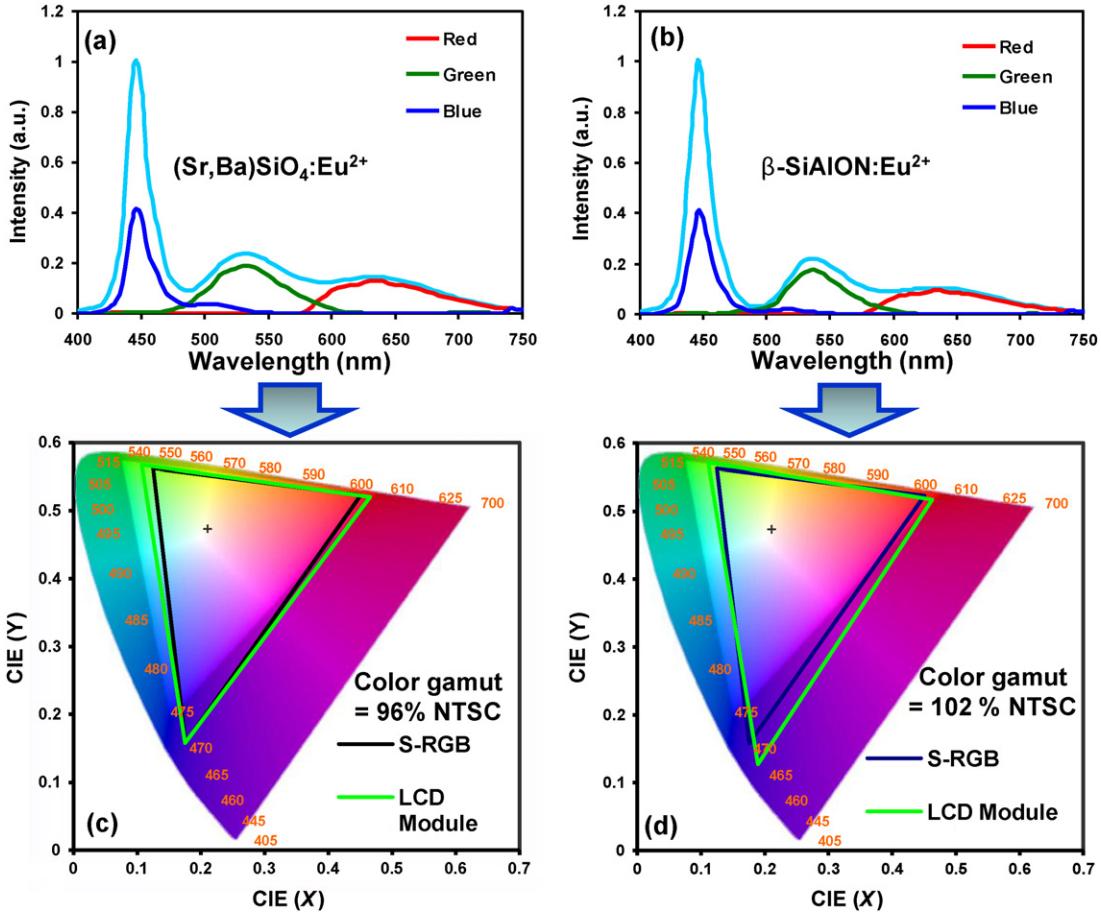

Fig. 4. White emission spectra and simulated results using commercial silicate green phosphor ($SrBaSiO_4:Eu^{2+}$) and β-SiAlON:Eu^{2+} are shown in (a) and (b). Color gamut values for the LED BLUs using two green phosphors are represented in (c) and (d), respectively. (For interpretation of the references to color in this figure legend, the reader is referred to the web version of this article.)

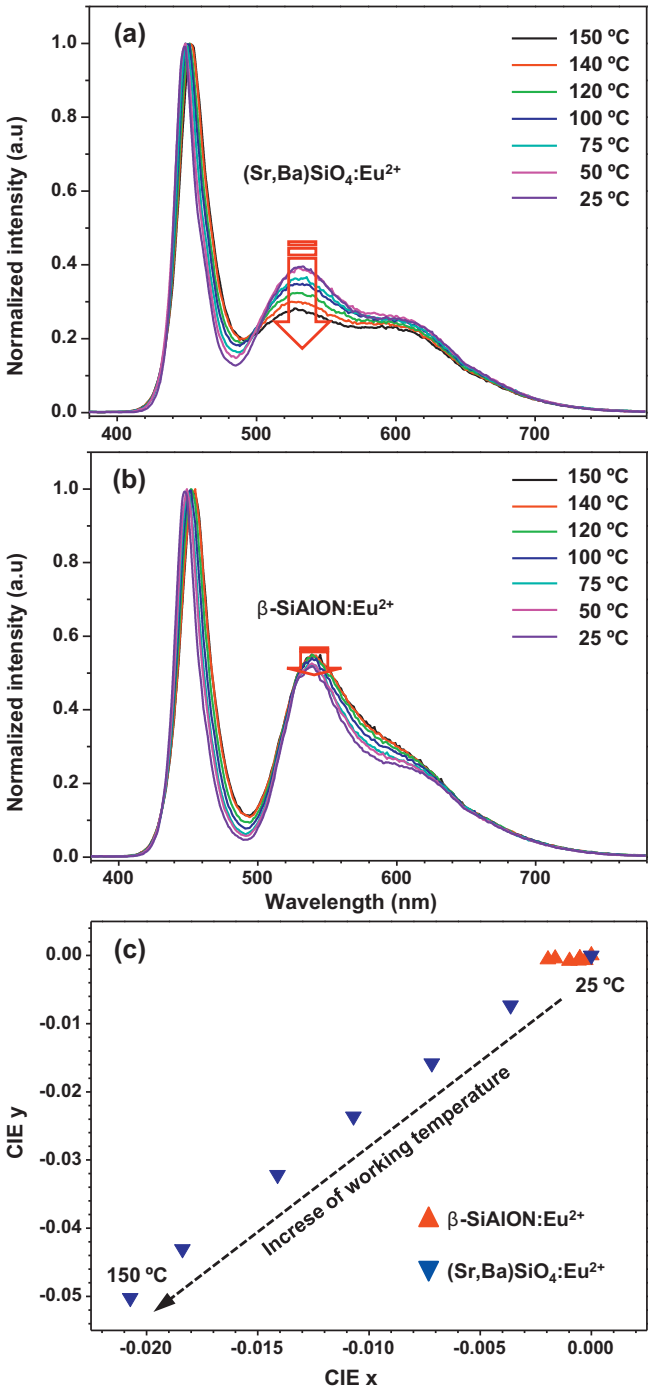

Fig. 5. Optical power-drop in white LEDs using (a) silicate ($SrBaSiO_4:Eu^{2+}$) and (b) β-SiAlON:Eu^{2+} for green phosphor according to working temperatures. Schematic diagram for the relation of working temperature with changes in chromaticity is depicted in (c).

and brightness-drop. These results can be attributed to the low thermal quenching property of the β-SiAlON:Eu^{2+} compared to silicate phosphor as proved in Fig. 3.

4. Conclusion

In this work, green emitting Eu^{2+}-doped β-SiAlON phosphor powder with a composition of $Eu_xSi_{6-z}Al_zO_yN_{8-y}$ ($y = z - 2x$, $x = 0.018$, $z = 0.23$) was successfully synthesized by gas pressured solid-state reaction for application to white LED. The prepared Eu^{2+}-doped β-SiAlON phosphor exhibited single emission band peaking at 538 nm excited at 450 nm. Using the electron-vibrational interaction of 4f-5d optical transitions in β-SiAlON:Eu^{2+} phosphor, as well as the temperature influence on the fitting of experimental emission spectra, the Stokes shift was calculated and the good agreement of the theory and experiment were realized. The thermal quenching properties of the prepared Eu^{2+}-doped β-SiAlON phosphor was superior to the silicate green phosphor, which means Eu^{2+}-doped β-SiAlON phosphor is promising for high-power LEDs. The white LED using the prepared β-SiAlON:Eu^{2+} green phosphor exhibited better stability in optical power and chromaticity compared to the silicate green phosphor in high working temperature. Moreover, the white LED using the prepared β-SiAlON:Eu^{2+} showed 102% of NTSC value in 1976 CIE color coordinate, which is 6% higher than the case using commercial silicate phosphor.

References

[1] B. Lee, S. Lee, H.G. Jeong, K.-S. Sohn, Solid-state combinatorial screening of $(Sr,Ca,Ba,Mg)_2Si_5N_8:Eu^{2+}$ phosphors, ACS Comb. Sci. 13 (2011) 154–158.

[2] T. Suehiro, N. Hirosaki, R.-J. Xie, Synthesis and photoluminescent properties of $(La,Ca)_3Si_6N_{11}:Ce^{3+}$ fine powder phosphors for solid-state lighting, ACS Appl. Mater. Interfaces 3 (2011) 811–816.

[3] T.-C. Liu, B.-M. Cheng, S.-F. Hu, R.-S. Liu, Highly stable red oxynitride β-SiAlON:Pr^{3+} phosphor for light-emitting diodes, Chem. Mater. 23 (2011) 3698–3705.

[4] S.T. Speers Jr., J.R. Perumareddi, A.W. Adamson, Crystal field energy levels for various symmetries, J. Phys. Chem. 72 (1968) 1822–1825.

[5] R.-J. Xie, N. Hirosaki, M. Mitomo, Y. Yamamoto, T. Suehiro, K. Sakuma, Optical properties of Eu^{2+} in α-SiAlON, J. Phys. Chem. B 108 (2004) 12027–12031.

[6] A. Rosenflanz, Silicon nitride and sialon ceramics, Curr. Opin. Solid State Mater. Sci. 4 (1999) 453–459.

[7] X.W. Zhu, Y. Masubuchi, T. Motohashi, S. Kikkawa, The z value dependence of photoluminescence in Eu^{2+}-doped β-SiAlON ($Si_{6-z}Al_zO_zN_{8-z}$) with $1 \le z \le 4$, J. Alloys Compd. 489 (2010) 157–161.

[8] J.H. Ryu, Y.-G. Park, H.S. Won, H. Suzuki, S.H. Kim, C. Yoon, Luminescent properties of β-SiAlON:Eu^{2+} green phosphors synthesized by gas pressured sintering, J. Ceram. Soc. Jpn. 116 (2008) 389–394.

[9] K. Kimoto, R.-J. Xie, Y. Matsui, K. Ishizuka, N. Hirosaki, Direct observation of single dopant atom in light-emitting phosphor of β-SiAlON:Eu^2, Appl. Phys. Lett. 94 (2009) 041908.

[10] A. Meijerink, G. Blasse, Luminescence properties of Eu^{2+}-activated alkaline earth haloborates, J. Lumin. 43 (1989) 283–289.

[11] I. Baginskiy, R.S. Liu, C.L. Wang, R.T. Lin, Y.J. Yao, Temperature dependent emission of strontium–barium orthosilicate ($Sr_{2-x}Ba_x$)-)$SiO_4:Eu^{2+}$ phosphors for high-power white light-emitting diodes, J. Electrochem. Soc. 158 (2011) P118–P121.

[12] Y. Peng, Z. Pei, G. Hong, Q. Su, Study on the reduction of $Eu^{3+} \rightarrow Eu^{2+}$ in $Sr_4Al_{14}O_{25}$:Eu prepared in air atmosphere, Chem. Phys. Lett. 371 (2003) 1–6.

[13] S. Shionoya, W.M. Yen, Phosphor Handbook, Laser & Optical Science & Technology Series, CRC, New York, 1998, pp. 35–48.

[14] J.H. Ryu, Y.-G. Park, H.S. Won, S.H. Kim, H. Suzuki, J.M. Lee, C. Yoon, M. Nazarov, D.Y. Noh, B. Tsukerblat, Luminescent properties of Ca-α-SiAlON:Eu^{2+} phosphors synthesized by gas-pressured sintering, J. Electrochem. Soc. 155 (2008) J99–J104.

[15] N. Narendran, Y. Gu, J.P. Freyssinier, H. Yu, L. Deng, Solid-state lighting: failure analysis of white LEDs, J. Cryst. Growth 268 (2004) 449–456.